—Note—

Postmortem magnetic resonance imaging findings of tricuspid atresia with ventricular and atrial septal defects and subvalvular pulmonic stenosis in a Japanese native Noma horse

Kenji KUTARA[1#*], Sho KADEKARU[1#], Keiichi HISAEDA[1], Keisuke SUGIMOTO[1], Tetsushi ONO[2], Yoichi INOUE[1], Shinichi NAKAMURA[1], Ryohei YOSHITAKE[1], Emi OHZAWA[3], Akira GOTO[1], Eri IWATA[1], Kenichi SHIBANO[1], Yumi UNE[1] and Hitoshi KITAGAWA[1]

[1]Faculty of Veterinary Medicine, Okayama University of Science, Ehime 794-8555, Japan
[2]Faculty of Veterinary Medicine, Yamaguchi University, Yamaguchi 753-8515, Japan
[3]Noma Horse Preservation Society, Ehime 794-0082, Japan

The necropsy of a 2-day-old Noma horse that died of weakness showed an enlarged cardiac base and a narrow cardiac apex, suggesting cardiac malformation. The excised heart underwent imaging to investigate its luminal structure. On three-dimensional magnetic resonance imaging, the right atrium and right ventricle were discontinuous. The right atrium communicated with the left atrium and the left ventricle communicated with the right ventricle. The lumen narrowed near the pulmonary artery valve. Since the same findings were observed on gross examination, the foal was diagnosed with tricuspid atresia with ventricular and atrial septal defects, along with subvalvular pulmonic stenosis.

Key words: *3D MRI, Noma horse, tricuspid atresia*

J. Equine Sci.
Vol. 34, No. 4
pp. 121–125, 2023

Tricuspid atresia, the congenital absence of the tricuspid valve, has been sporadically reported in horses, mostly in Arab or Arab-bred foals [2, 4, 7–10, 12, 16, 20, 21]. The etiology of tricuspid atresia is likely multifactorial, involving environmental and genetic factors; however, no specific risk factors have been identified in humans or animals [18]. In humans, magnetic resonance imaging (MRI) is clinically applied because it simultaneously displays the inside and outside of the heart. This makes it more suitable than X-ray angiography or echocardiography for imaging cardiac structures [6, 11]. However, in veterinary medicine, cardiac MRI can be challenging due to anesthesia-induced immobilization and variations in animal body size. Postmortem imaging has garnered attention in human forensic medicine for aiding the diagnosis of sudden death by visualizing cardiovascular abnormalities [1, 3, 13]. This report describes a postmortem MRI performed on the heart of a Noma horse foal that died suddenly. This enabled the diagnosis of structural cardiac abnormalities by reconstructing the heart in 3D.

The foal was a 2-day-old Noma horse that died of frailty. The foal had stood and nursed on the day of birth. On the day after birth, the foal showed lethargy and weakness, and it was unable to stand. It was therefore examined by veterinarians that day. Hypothermia (rectal temperature, 37.2°C) and aperture were noted. The heart and respiratory rates were 124 beats per minute and 18 breaths per minute, respectively. The mucous membranes were moist, and cyanosis was not evident. A provisional diagnosis of hypothermia due to inadequate lactation was made. The foal was treated with force-feeding and warming measures; however, it died the next day.

The body of the foal was transported for necropsy to the Faculty of Veterinary Medicine, Okayama University of Science, Imabari, Japan, within 1 hr of death. The visible mucosae were cyanotic. On necropsy, the abdominal organs

Received: July 14, 2023
Accepted: September 1, 2023
*Corresponding author. e-mail: k-kutara@ous.ac.jp
#These authors contributed equally to this work.

showed no specific abnormalities. The lungs were diffusely dark pink in color with mild pulmonary edema. A subjective evaluation of the heart revealed that it was larger at the base and narrower at the apex (Fig. 1A). The anterior interventricular groove was also shifted to the right. The caudal vena cava was thin, and hypoplasia was suspected. Because a cardiac malformation was suspected, the heart was removed from the body, and it was found to weigh 202.7 g, representing 1.35% of the total body weight. It was then directly immersed in formalin in an acrylic container.

To observe the 3D luminal structure of the heart, MRI was performed using a 1.5T superconducting unit (Vantage Elan, Canon Medical Systems, Otawara, Japan) 2 days after fixation in formalin. For MRI, 3D T1-weighted image (T1WI) and T2-weighted image (T2WI) scans were acquired. The sequence parameters were as follows: FASE, TR/TE = 550/15 msec, spatial resolution = 0.7 × 0.7 mm, and slice thickness = 1.0 mm for 3D T1WI; FASE, TR/TE = 2,000/35.2 msec, spatial resolution = 0.7 × 0.7 mm, and slice thickness = 1.0 mm for 3D T2WI. For all sequences, the field-of-view size was fixed at 180 × 180 mm. A workstation (VAZE, Pet Communications, Osaka, Japan) was used for multiplanar reconstruction (MPR; Figs. 1B and 2) and 3D reconstruction of all MRI images (Figs. 1C and 3).

The MRI images revealed that the right atrium and ventricle were separated by a wall, but the tricuspid valve could not be observed (Figs. 2A and 3). Additionally, the right ventricle was small, with a narrowed lumen near the pulmonary artery valve (inner diameter, 2 mm; Figs. 2B and 3). No wall separating the right and left ventricles was observed ventral to the aortic valve (Figs. 1B and 2B). The ventricular septum was very thin and membranous. An interatrial communication was observed, indicating a patent foramen ovale. The pulmonary artery and aorta lumens were clearly visible, and no stenosis was observed. No dilatation of the ductus arteriosus was observed (inner diameter, 2 mm). The cranial vena cava was dilated, and the caudal vena cava was thinner than expected.

Based on the 3D MRI findings, a heart dissection was performed. The heart luminal structures were similar to those observed on MRI (Fig. 4). The tricuspid orifice showed no evidence of a valve. A novel finding was that the pulmonary artery valve comprised two semilunar valves (Fig. 4C). The mitral valve showed no obvious abnormalities.

The cardiac diagnoses for this foal were as follows: tricuspid atresia, accompanied by ventricular and atrial septal defects, and subvalvular pulmonic stenosis. Tricuspid atresia is classified according to the morphology of the tricuspid valve, the position of the aorta, and pulmonary artery pathology [15, 18, 20]. In this case, no membrane-like structures were observed between the right atrium and ventricle, and each was shown to be an independent luminal structure covered by muscle. After describing the morphology of the tricuspid valve, tricuspid atresia was further classified according to the relationship between the associated great vessels (the aorta and pulmonary artery) [14]. In this case, tricuspid atresia was type I-b, which is the most common form in humans [14]. Tricuspid atresia

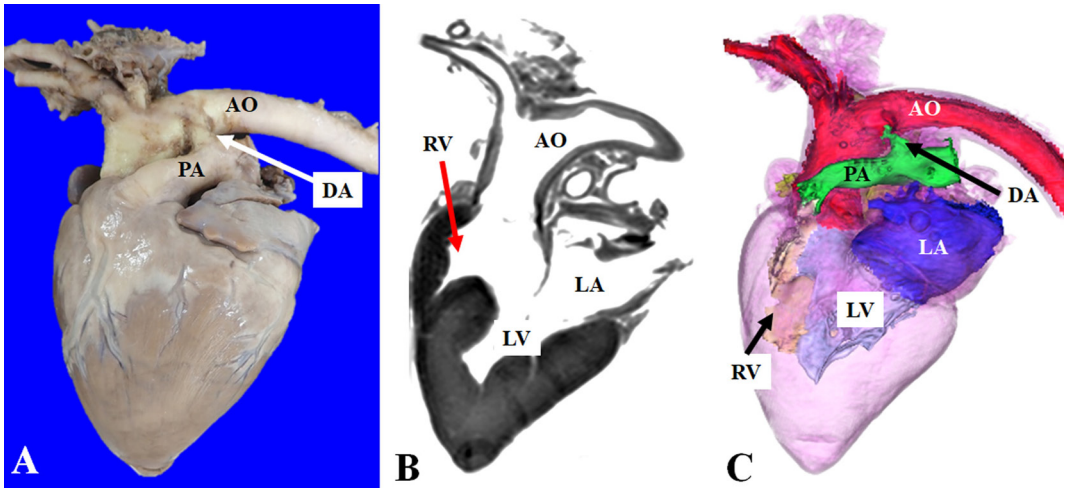

Fig. 1. Three different views of the heart. (A) Left appearance of the heart. The heart appeared to have a large cardiac base and narrow cardiac apex. The anterior interventricular groove was shifted to the right. (B) MRI in the sagittal plane at the level of the aortic valve. No wall separating the right and left ventricles was observed ventral to the aortic valve. (C) Appearance of the left side of the heart in a 3D image reconstructed from MRI. The myocardial portion was made more permeable so that the luminal structure could be observed. The lumen of the ductus arteriosus was narrow. AO, aorta; DA, ductus arteriosus; LA, left atrium; LV, left ventricle; MRI, magnetic resonance imaging; PA, pulmonary artery; RV, right ventricle.

type I-b is characterized by a normal relationship between the great vessels (type I) and the presence of pulmonary stenosis or hypoplasia (subtype b).

In tricuspid atresia, because the right atrium and right ventricle are not continuous, blood cannot flow normally into the right outflow tract. Thus, for venous blood to return to the right atrium to be shunted to the left atrium, left ventricle, and aorta, interventricular communication in the form of atrial (e.g., foramen ovale patency) and ventricular septal defects is necessary for survival. A connection between the right outflow tract and pulmonary circulation must occur via one of three pathways: a ventricular septal defect, the ductus arteriosus, or aortopulmonary collaterals. In this case, the foal exhibited atrial and ventricular septal defects. Postnatal survival was possible because venous blood flowed through these two defects into the left outflow tract and the pulmonary artery. The magnitude of pulmonary blood flow depends largely on the degree of pulmonary outflow obstruction. In cases of pulmonary atresia or stenosis, pulmonary blood flow is reduced with narrowing

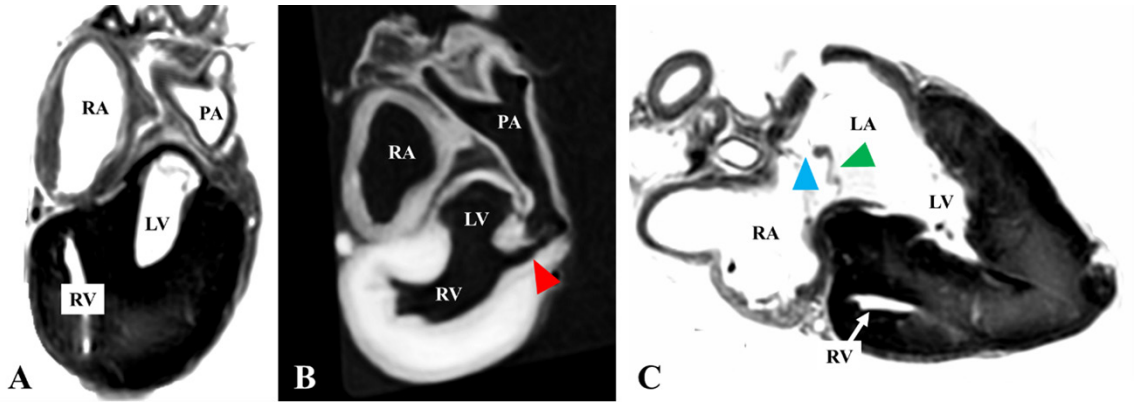

Fig. 2. Multiplanar reconstructed MRI. (A) T2-weighted image in the axial plane at the level of the right ventricle. The right atrium and right ventricle were separated by a wall, and the tricuspid valve was not seen. (B) T1-weighted image in the axial plane at the level of the pulmonary artery. The lumen was narrow near the pulmonary artery valve (red arrowhead). No separating wall was observed between the right and left ventricles. (C) T2-weighted image in the four-chamber plane created by multiplanar reconstruction. A traffic channel was present between the right and left atria (blue arrowhead). A very thin membranous structure (green arrowhead), potentially indicative of an atrial septum, was seen ventrally. LA, left atrium; LV, left ventricle; MRI, magnetic resonance imaging; PA, pulmonary artery; RA, right atrium; RV, right ventricle.

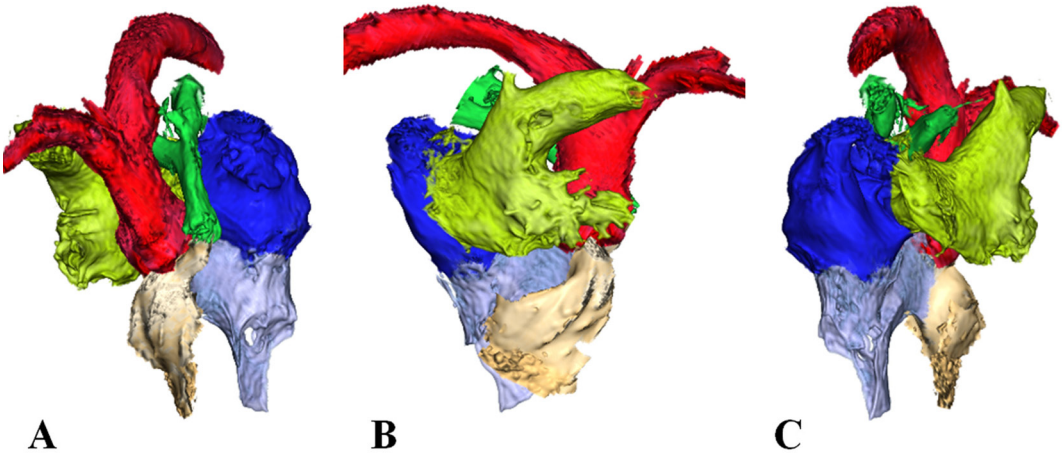

Fig. 3. 3D images of the heart lumen reconstructed from magnetic resonance imaging. (A) Cranial appearance. (B) Right appearance. (C) Caudal appearance. The right atrium and ventricle were not continuous. The right atrium communicated with the left atrium, and the left ventricle communicated with the right ventricle. This allowed venous blood returning to the right atrium to shunt to the left atrium, left ventricle, and aorta. Red region, aorta; green region, pulmonary artery; dark blue region, left atrium; light blue region, left ventricle; yellow region, right atrium; pale orange region, right ventricle.

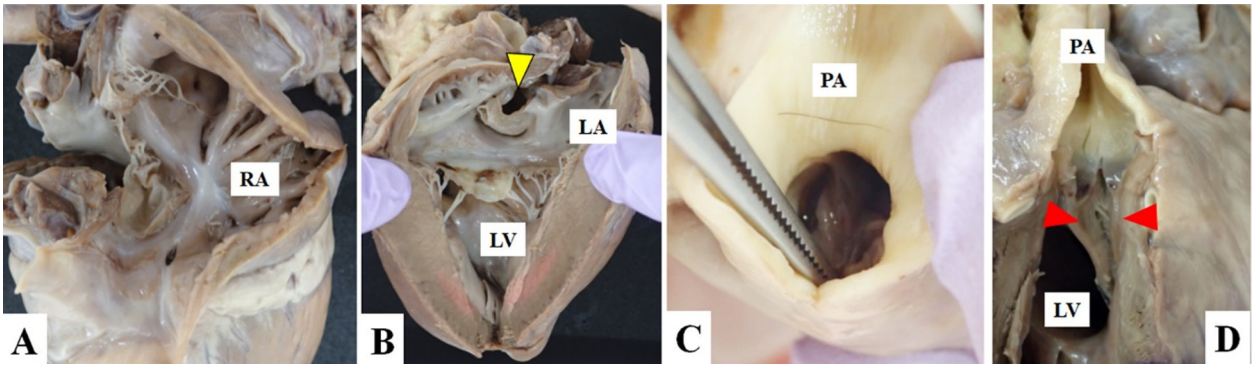

Fig. 4. Postmortem images of the heart lumens. (A) Image of the lumen of the right atrium. There was no evidence of a tricuspid valve or valve mouth formation between the right ventricle and right atrium. (B) Image of the lumens of the left atrium and left ventricle. The foramen ovale was partially covered by a fenestrated membrane with an uncovered dorsal rim (yellow arrowhead). The left and right atria were therefore continuous. (C) Image of the pulmonary artery valve. The pulmonary artery valve comprised two semilunar valves. (D) Image of the lumen of the right ventricle. The lumen was narrow near the pulmonary artery valve (red arrowheads). A communication opening was observed in the left ventricle. LA, left atrium; LV, left ventricle; PV, pulmonary artery; RA, right atrium; RV, right ventricle.

or occlusion of the ductus arteriosus, and the degree of cyanosis worsens. In the present case, the ductus arteriosus narrowed, which may have exacerbated the symptoms.

In this case, the morphological structure of the cardiac malformation could be understood in 3D by postmortem MRI. Postmortem imaging, particularly MRI, has emerged as a useful adjunct tool to autopsies in cardiac evaluation [1, 3, 13, 17, 19]. This technique has the potential to contribute significantly to veterinary medicine research and knowledge advancement. Postmortem imaging offers the advantage of reusing data from autopsies, allowing for arbitrary display of cross-sections through multi-planar and 3D reconstruction. This capability enhances anatomical understanding, ultrasound examination training, and surgical simulation beyond the limitations of two-dimensional and localized autopsy photographs.

Postmortem MRI can provide 3D information of the heart, even after formalin immersion (as in this case), allowing data acquisition when abnormalities are identified at necropsy. Studies in which the hearts of patients who died suddenly were fixed in formalin and subjected to MRI have also reported the utility of postmortem MRI for forensic diagnosis in humans [1, 3]. The ability to perform MRI after formalin fixation has the potential to overcome logistical challenges in body transportation, including time constraints due to postmortem changes and geographical limitations related to the installation of facilities.

This case report has some limitations. First, because MRI was performed after necropsy, whether or not there were any non-cardiac vascular abnormalities remains unknown. Second, it has been reported that formalin-fixed hearts show shortened T1 and T2 values [5]. Therefore, myocardial degeneration could not be investigated using MRI.

In conclusion, this 3D MRI study presents the structure of tricuspid atresia in the heart of a Noma horse with ventricular and atrial septal defects, along with subvalvular pulmonic stenosis. Reconstruction of the structure of the heart in 3D easily reveals the relationships between the ventricles and the location of the great vessels.

Funding

This research received no external funding.

Conflicts of Interest

The authors have no conflicts of interest to disclose.

Acknowledgments

We thank the staff of Imabari Nomauma Highland and the staff of the Imabari City Office for their contributions.

References

1. Aquaro, G.D., Guidi, B., Emdin, M., Pucci, A., Chiti, E., Santurro, A., Scopetti, M., Biondi, F., Maiese, A., Turillazzi, E., Camastra, G., Faggioni, L., Cioni, D., Fineschi, V., Neri, E., and Di Paolo, M. 2022. Post-mortem cardiac magnetic resonance in explanted heart of patients with sudden death. *Int. J. Environ. Res. Public Health* **19**: 13395. [Medline] [CrossRef]
2. Bayly, W.M., Reed, S.M., Leathers, C.W., Brown, C.M., Traub, J.L., Paradis, M.R., and Palmer, G.H. 1982. Multiple congenital heart anomalies in five Arabian foals. *J.*

Am. Vet. Med. Assoc. **181**: 684–689. [Medline]
3. Bertozzi, G., Cafarelli, F.P., Ferrara, M., Di Fazio, N., Guglielmi, G., Cipolloni, L., Manetti, F., La Russa, R., and Fineschi, V. 2022. Sudden cardiac death and ex-situ postmortem cardiac magnetic resonance imaging: a morphological study based on diagnostic correlation methodology. *Diagnostics (Basel)* **12**: 218. [Medline] [CrossRef]
4. Button, C., Gross, D.R., Allert, J.A., and Kitzman, J.V. 1978. Tricuspid atresia in a foal. *J. Am. Vet. Med. Assoc.* **172**: 825–830. [Medline]
5. Ebata, K., Noriki, S., Inai, K., and Kimura, H. 2021. Changes in magnetic resonance imaging relaxation time on postmortem magnetic resonance imaging of formalin-fixed human normal heart tissue. *BMC Med. Imaging* **21**: 134. [Medline] [CrossRef]
6. Fletcher, B.D., Jacobstein, M.D., Abramowsky, C.R., and Anderson, R.H. 1987. Right atrioventricular valve atresia: anatomic evaluation with MR imaging. *AJR Am. J. Roentgenol.* **148**: 671–674. [Medline] [CrossRef]
7. Gumbrell, R.C. 1970. Atresia of the tricuspid valve in a foal. *N. Z. Vet. J.* **18**: 253–256. [Medline] [CrossRef]
8. Hall, T.L., Magdesian, K.G., and Kittleson, M.D. 2010. Congenital cardiac defects in neonatal foals: 18 cases (1992–2007). *J. Vet. Intern. Med.* **24**: 206–212. [Medline] [CrossRef]
9. Kohnken, R., Schober, K., Godman, J., Gardner, A., Jenkins, T., Schroeder, E., Baker, P., and Dunbar, L. 2018. Double outlet right ventricle with subpulmonary ventricular septal defect (Taussig-Bing anomaly) and other complex congenital cardiac malformations in an American Quarter Horse foal. *J. Vet. Cardiol.* **20**: 64–72. [Medline] [CrossRef]
10. Krüger, M.U., Wünschmann, A., Ward, C., and Stauthammer, C.D. 2016. Pulmonary atresia with intact ventricular septum and hypoplastic right ventricle in an Arabian foal. *J. Vet. Cardiol.* **18**: 284–289. [Medline] [CrossRef]
11. Mayo, J.R., Roberson, D., Sommerhoff, B., and Higgins, C.B. 1990. MR imaging of double outlet right ventricle. *J. Comput. Assist. Tomogr.* **14**: 336–339. [Medline] [CrossRef]
12. Meurs, K.M., Miller, M.W., Hanson, C., and Honnas, C. 1997. Tricuspid valve atresia with main pulmonary artery atresia in an Arabian foal. *Equine Vet. J.* **29**: 160–162. [Medline] [CrossRef]
13. Michaud, K., Jacobsen, C., Basso, C., Banner, J., Blokker, B.M., de Boer, H.H., Dedouit, F., O'Donnell, C., Giordano, C., Magnin, V., Grabherr, S., Suvarna, S.K., Wozniak, K., Parsons, S., and van der Wal, A.C. 2023. Application of postmortem imaging modalities in cases of sudden death due to cardiovascular diseases–current achievements and limitations from a pathology perspective : endorsed by the Association for European Cardiovascular Pathology and by the International Society of Forensic Radiology and Imaging. *Virchows Arch.* **482**: 385–406. [Medline] [CrossRef]
14. Minocha, P.K., and Phoon, C. 2023. Tricuspid atresia. *In*: StatPearls [Internet], StatPearls Publishing, Treasure Island.
15. Rao, P.S. 1992. Classification of tricupsid atresia. pp. 59–77. *In*: Tricuspid Atresia, 2nd ed. (Rao, P.S. ed.), Futura Publishing Company Inc., New York.
16. Reef, V.B., Mann, P.C., and Orsini, P.G. 1987. Echocardiographic detection of tricuspid atresia in two foals. *J. Am. Vet. Med. Assoc.* **191**: 225–228. [Medline]
17. Shelmerdine, S.C., Sebire, N.J., and Arthurs, O.J. 2021. Diagnostic accuracy of postmortem ultrasound vs postmortem 1.5-T MRI for non-invasive perinatal autopsy. *Ultrasound Obstet. Gynecol.* **57**: 449–458. [Medline] [CrossRef]
18. Slack, J., Johns, I., Van Eps, A., and Reef, V.B. 2008. Imaging diagnosis–tricuspid atresia in an alpaca. *Vet. Radiol. Ultrasound* **49**: 309–312. [Medline] [CrossRef]
19. Tang, H., Zhang, Y., Dai, C., Ru, T., Li, J., Chen, J., Zhang, B., Zhou, K., Lv, P., Liu, R., Zhou, Q., and Zheng, M. 2022. Postmortem 9.4-T MRI for fetuses with congenital heart defects diagnosed in the first trimester. *Front. Cardiovasc. Med.* **8**: 764587. [Medline] [CrossRef]
20. van der Linde-Sipman, J.S., and van den Ingh, T.S. 1979. Tricuspid atresia in a foal and a lamb. *Zentralbl. Veterinärmed. A* **26A**: 239–242. [Medline]
21. Zamora, C.S., Vitums, A., Nyrop, K.A., and Sande, R.D. 1989. Atresia of the right atrioventricular orifice with complete transposition of the great arteries in a horse. *Anat. Histol. Embryol.* **18**: 177–182. [Medline] [CrossRef]